

The effect of size factor on the phase transition in $\text{Sn}_2\text{P}_2\text{S}_6$ crystals: experimental data and simulation in ANNNI model

A.V.Drobnich¹, A.A.Molnar¹, A.V.Gomonnai²,
Yu.M.Vysochanskii¹, I.P.Prits¹

¹ Uzhhorod National University, 46 Pidhirna Str., 88000 Uzhhorod, Ukraine

² Institute of Electron Physics
of the National Academy of Sciences of Ukraine,
21 Universytetska Str., 88000 Uzhhorod, Ukraine

Received October 18, 2002, in final form April 21, 2003

Size effect on the fundamental properties of $\text{Sn}_2\text{P}_2\text{S}_6$ ferroelectric is studied. The decrease of Raman peak frequency, accompanied by the band broadening and asymmetry, is observed in the spectra of microcrystalline $\text{Sn}_2\text{P}_2\text{S}_6$ powder. Theoretical calculations, performed in the ANNNI model for $\text{Sn}_2\text{P}_2\text{S}_6$ microcrystals of different size, predict the decrease of the ferroelectric phase transition temperature with the decrease of the microcrystal size parameter.

Key words: *microcrystals, size effects, Raman scattering, ANNNI model*

PACS: *36.40.Ei, 63.22.+m*

1. Introduction

Changes of ferroelectric phase transition (PT) parameters with the sample size decrease from bulk to microcrystals have been reported for oxygen-containing ferroelectrics PbTiO_3 [1,2], NaNNO_2 [3], KH_2PO_4 [3], BaTiO_3 [4]. Tin hexathiohypodiphosphate $\text{Sn}_2\text{P}_2\text{S}_6$ is a model ferroelectric crystal, where at 337 K a second-order structural phase transition $\text{P}2_1/c \Rightarrow \text{P}c$ occurs [5]. For $\text{Sn}_2\text{P}_2\text{S}_6$ microcrystal-based ceramics, the PT temperature was observed to decrease with respect to that of the bulk sample [6]. Therefore, it seemed interesting to perform experimental studies of Raman scattering in microcrystalline $\text{Sn}_2\text{P}_2\text{S}_6$ as well as theoretical simulation of the size effect on the PT parameters.

2. Size effect in Raman scattering spectra

The objects of our study were $\text{Sn}_2\text{P}_2\text{S}_6$ microcrystals with average size of $10\ \mu\text{m}$, obtained by milling the single crystals, grown by chemical vapour method. Both powder samples as well as $\text{Sn}_2\text{P}_2\text{S}_6$ ceramics, fabricated from these microcrystals with a technique similar to that of [6], were used for Raman measurements. The spectra were recorded on a LOMO DFS-24 double grating monochromator at room temperature, the excitation being provided by He-Ne laser ($632.8\ \text{nm}$).

$\text{Sn}_2\text{P}_2\text{S}_6$ is known to possess a rich phonon spectrum, reported in detail in [7]. We focus our attention on one of the most pronounced Raman peaks, corresponding to the vibration of P–P bonds, linking two pyramid-shaped PS_3 structural groups, whose frequency at room temperature is $381.4\ \text{cm}^{-1}$ for bulk single crystals. As it is seen in figure 1, in powdered microcrystalline $\text{Sn}_2\text{P}_2\text{S}_6$ the peak frequency shifts down to $380.2\ \text{cm}^{-1}$, which is accompanied by the band broadening (from 6 to $8\ \text{cm}^{-1}$ FWHM) and asymmetry. Note that in $\text{Sn}_2\text{P}_2\text{S}_6$ ceramics, the peak position frequency practically does not decrease ($381.3\ \text{cm}^{-1}$) and no band broadening is observed (figure 1c).

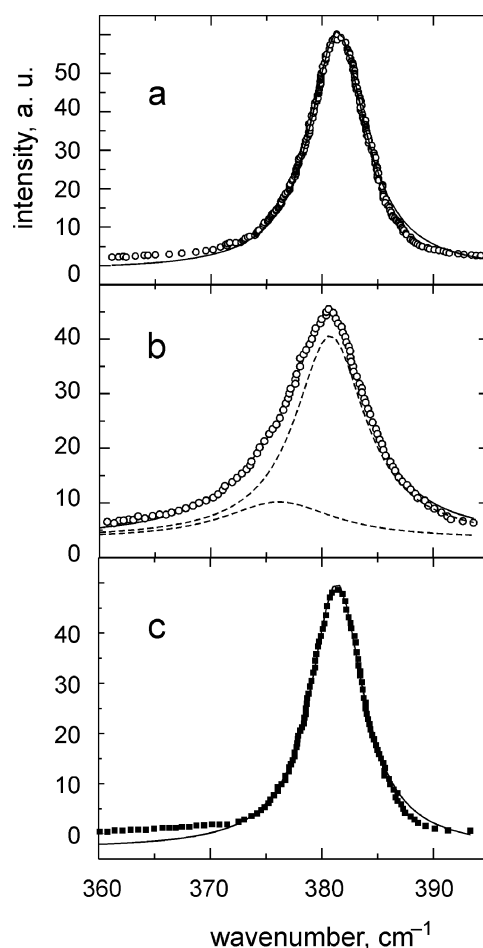


Figure 1. Raman lineshape of the P–P vibration band in the spectrum of bulk (a), $10\text{-}\mu\text{m}$ powder (b) and ceramic (c) $\text{Sn}_2\text{P}_2\text{S}_6$.

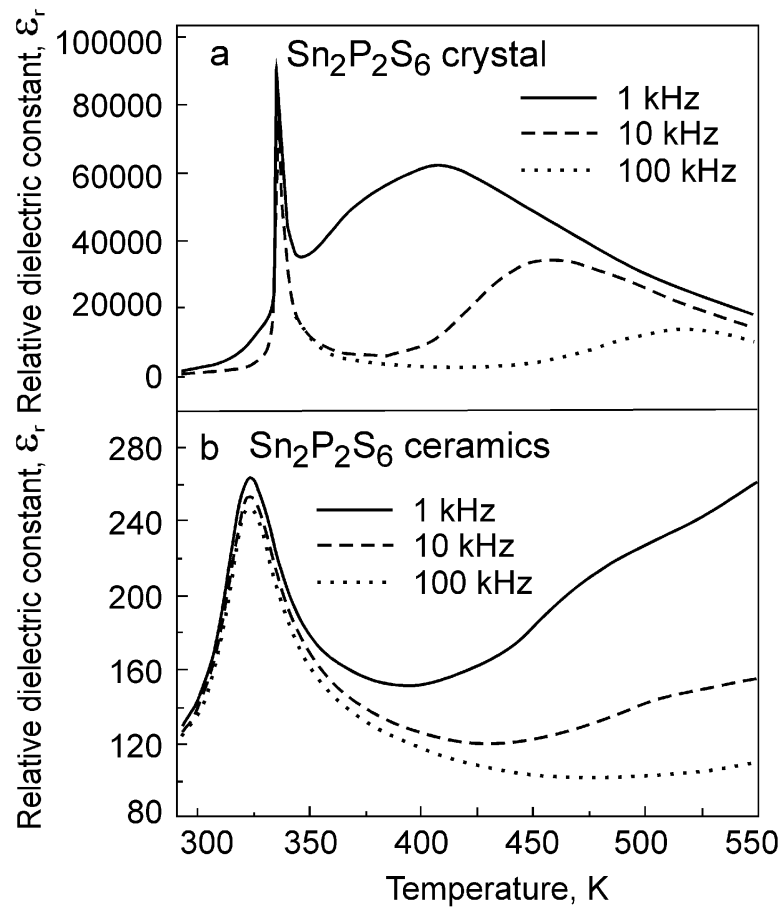


Figure 2. Temperature dependences of the dielectric constant at different frequencies for $\text{Sn}_2\text{P}_2\text{S}_6$ crystal (a) and ceramics (b) [6].

Similar features (Raman peak frequency decrease, broadening and asymmetry, which are generally more pronounced at the crystal size decrease) have been observed earlier for the Raman spectra of microcrystalline Si, III-V and II-VI semiconductors [8–10] where they are explained by two main factors: (i) confinement-related selection rules relaxation and contribution of $q \neq 0$ phonons due to the small crystallite size and (ii) surface phonon modes whose role in the Raman spectrum increases in microcrystals due to much higher surface-to-volume ratio.

Since in our case, contrary to some other Raman bands in $\text{Sn}_2\text{P}_2\text{S}_6$ [11], the P–P bond vibration frequency remains practically unchanged across the Brillouin zone [12], the contribution of the confinement-related factor can be neglected and the experimentally observed features can be attributed to surface effects. Hence, the experimental spectra can be simulated by a superimposition of two Lorentzian contours (dashed line), corresponding to the bulk and surface phonons whose frequencies are 380.8 and 377.0 cm^{-1} with the bandwidths 7.5 and 12 cm^{-1} , respectively (figure 1b). As concerns the $\text{Sn}_2\text{P}_2\text{S}_6$ ceramics (figure 1c), the role of surface phonons here is obviously much smaller, which is probably related to the features of dynamics at the interfaces between the microcrystalline grains in the ceramic sample.

The temperature dependence of the relative dielectric constant for $\text{Sn}_2\text{P}_2\text{S}_6$ single crystal (figure 2) has, at the second order phase transition close to 337 K, a sharp anomaly, with the value in the maximum close to 9×10^4 . The ceramic sample shows a broad anomaly with much lower maximum value (near 250–265) than in the single crystal. The transition temperature in the ceramics is observed at 325 K. These differences between the ceramics and the single crystal dielectric properties are due to the grain size effect. In the ceramic sample, the average grain size is smaller than $1 \mu\text{m}$. So, for the $\text{Sn}_2\text{P}_2\text{S}_6$ ferroelectric, as in the case of other ferroelectric compounds [1–4], when the grain size decreases, the dielectric anomaly during the phase transition becomes broad, the maximum of the dielectric constant at T_0 decreases, and the transition temperature shifts down.

3. Monte Carlo simulations of the size effect

For the research of PTs in microcrystals an ANNNI (axial next nearest neighbour Ising) model is widely used [14,15]. In the framework of this model such effects as the dependence of temperature of the bulk PT between the ferroelectric and paraelectric phases on the size parameter of a model lattice, the effect of the microscopic sample surface on the phase transformations were demonstrated. We use here the ANNNI model in order to relate a known abstract model to an actual phase diagram of microcrystals such as $\text{Sn}_2\text{P}_2\text{S}_6$.

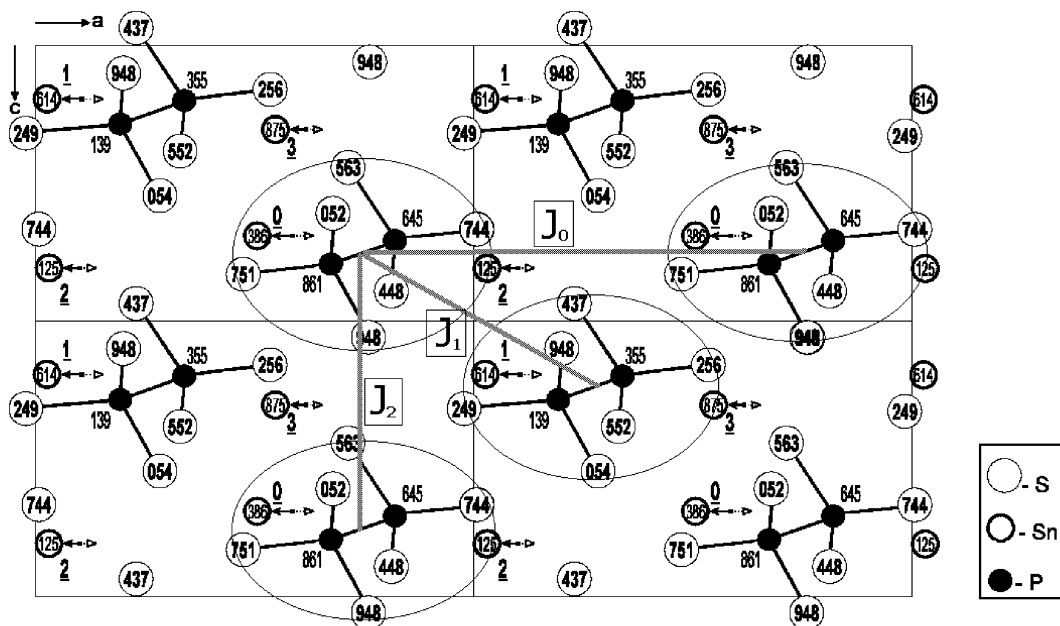


Figure 3. The projection of $\text{Sn}_2\text{P}_2\text{S}_6$ crystal structure in the ferroelectric phase on the (010) plane. The altitude of the atoms is indicated in millesimals of the lattice period. The arrows mark the atoms of the ferroelectric sublattice.

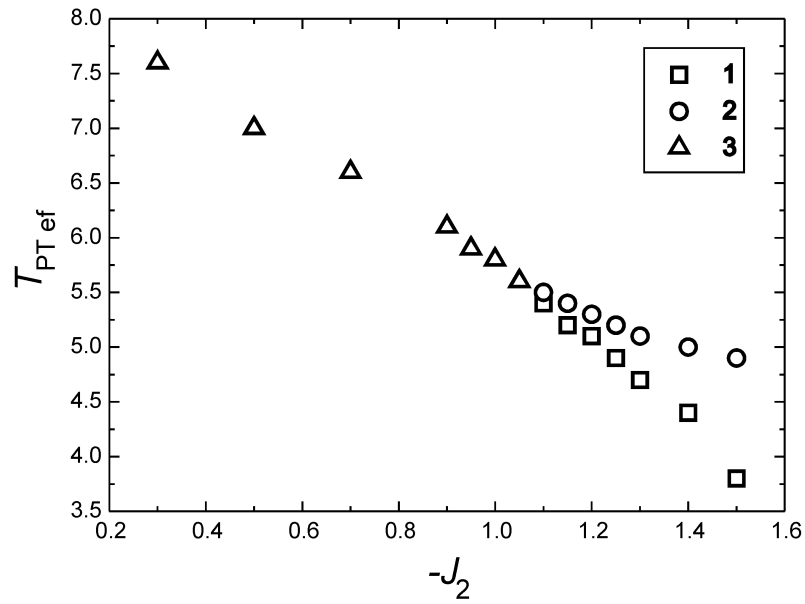


Figure 4. The phase diagram of the ANNNI-adapted model in the vicinity of the Lifshitz point at $J_0 = J_1 = 1$: 1 – PT from incommensurate (IC) to ferroelectric (FE) phase, 2 – PT from paraelectric (PE) to incommensurate (IC) phase, 3 – PT from paraelectric (PE) to ferroelectric (FE) phase.

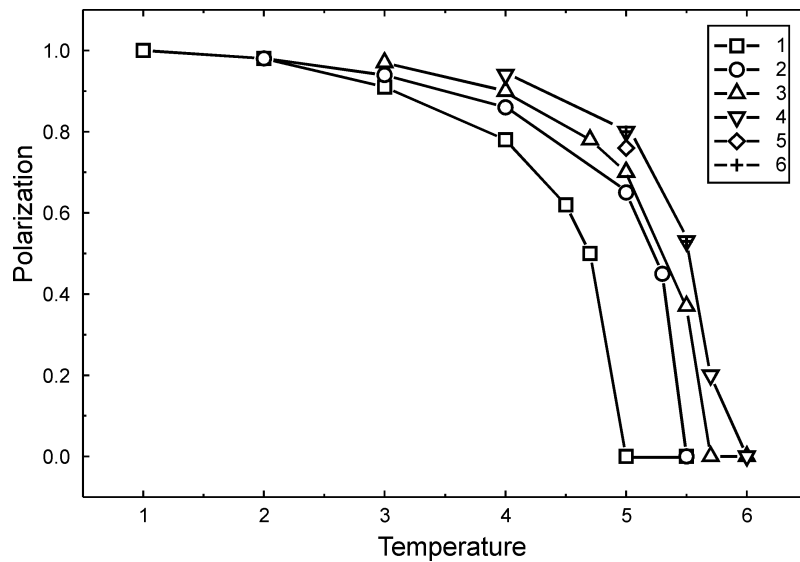


Figure 5. The results of the MC calculations of bulk $\text{Sn}_2\text{P}_2\text{S}_6$ polarization (MC cell with PBC) and of microscopic $\text{Sn}_2\text{P}_2\text{S}_6$ polarization (MC cell with free boundary conditions) in the ANNNI-adapted model: 1 – $9 \times 9 \times 9$ MC cell, 2 – $17 \times 17 \times 17$ MC cell, 3 – $33 \times 33 \times 33$ MC cell, 4 – $17 \times 17 \times 17$ MC cell with PBC, 5 – $67 \times 67 \times 67$ MC cell, 6 – $67 \times 67 \times 67$ MC cell with PBC.

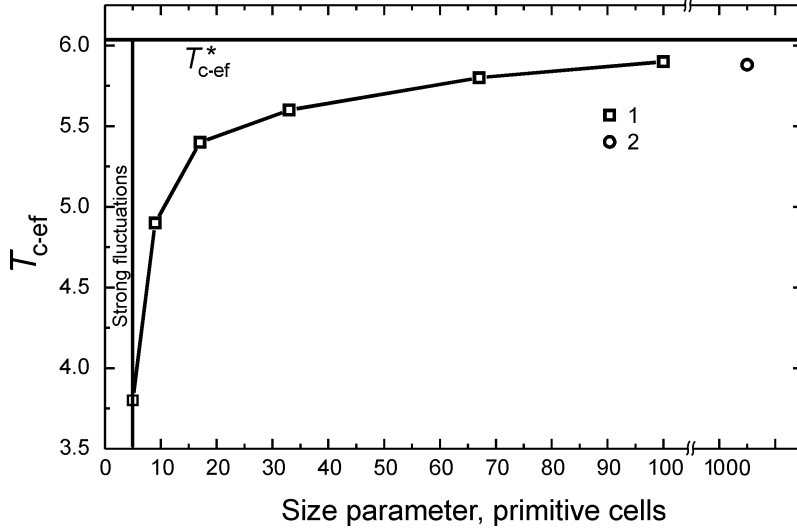


Figure 6. Dependence of T_{c-ef} on the size parameter of the microcrystal model: 1 – data of MC calculation, 2 – data of physical experiment. The value of T_{c-ef}^* is obtained in MC cell with PBC for the bulk crystal.

We shall link an effective dipole to a molecular group of atoms $\text{Sn}_2\text{P}_2\text{S}_6$ (four such groups are marked in figure 3 by ellipses), its electrical dipolar moment being directed along the \mathbf{a} axis. From the scheme of concurrent interactions in the framework of the ANNNI model we determine the interactions in our model. They are represented by coefficients $J_0 > 0$ – between the dipoles located on the \mathbf{a} axis, $J_1 > 0$ – between the nearest adjacent dipoles, $J_2 < 0$ – between the nearest dipoles with negative interaction. For simplicity we assume $J_0 = J_1 = 1$.

Contrary to the earlier work [14] where the phase diagram of the ANNNI model for a cubic lattice was obtained by the mean-field method, here we specify the coefficients of the adapted ANNNI model more exactly with respect to the $\text{Sn}_2\text{P}_2\text{S}_6$ crystal lattice. We have constructed an exact phase diagram in the vicinity of the Lifshitz point by a Monte Carlo (MC) method (figure 4).

The boundary conditions used for the calculations deserve special consideration. For the simulation of the bulk crystal we have used periodic boundary conditions (PBC), for the microcrystals – free boundary conditions.

The coefficients for the $\text{Sn}_2\text{P}_2\text{S}_6$ model can be evaluated by the comparison of the experimental diagram of $\text{Sn}_2\text{P}_2(\text{S}_{1-x}\text{Se}_x)_6$ solid solutions [5,13] with the calculated one, shown in figure 4, and using the proportionality of J_2 and x . For $x = 1$ ($\text{Sn}_2\text{P}_2\text{Se}_6$ compound) the temperature width of the incommensurate (IC) phase is $(T_i - T_c)/T_i \sim 0.13$ and at $x = 0.28$ (Lifshitz point) the IC phase disappears. Hence, $J_2 = -1.05$ for $x = 0$ is determined.

We have performed a series of numerical tests within the ANNNI-adapted model with the obtained parameters for various sizes of the Monte Carlo cell, the results being shown in figure 5. Temperature is usually characterized by the effective temperature $T_{ef} = abckT/M_0^2$ where a, b, c are the unit cell parameters, k is the Boltzmann constant, M_0 is the effective dipolar moment, related to the dipolar moment μ as

$\mu = M_0 m_j$, $m_j = \pm 1$ are the Ising variables. As it is seen in figure 6, the calculated effective temperature $T_{c\text{-ef}}$ of the ferroelectric-to-paraelectric phase transition increases with the size parameter with subsequent saturation, obtained within the model with PBC, i.e. the models for bulk $\text{Sn}_2\text{P}_2\text{S}_6$. These results are in a qualitative agreement with the experimental data [6].

ANNNI is a well studied theoretical model. The fact that this model has been applied to $\text{Sn}_2\text{P}_2\text{S}_6$ crystal, enables a number of properties, predicted by this model, to be foreseen for the material under investigation. For example, the ANNNI model predicts a surface PT in $\text{Sn}_2\text{P}_2\text{S}_6$. In [15] the phase diagram with surface interaction coefficients was calculated by a cluster algorithm. This approach can be used for the search of surface PT in $\text{Sn}_2\text{P}_2\text{S}_6$ thin films.

4. Conclusions

The performed experimental and theoretical studies have shown the fundamental properties of $\text{Sn}_2\text{P}_2\text{S}_6$ ferroelectric to vary in case the crystal size parameter decreases from bulk to microcrystalline samples. The downward shift of Raman peak frequency, accompanied by the band broadening and asymmetry, is observed in the spectra of microcrystalline $\text{Sn}_2\text{P}_2\text{S}_6$ powder. The theoretical calculations, performed in the ANNNI model for $\text{Sn}_2\text{P}_2\text{S}_6$ microcrystals of different size, predict the decrease of the ferroelectric phase transition temperature with the decrease of the microcrystal size parameter.

5. Acknowledgement

The authors are grateful to Yu.Azhniuk for helpful discussions.

References

1. Ishikawa K., Yoshikawa K., Okada N. // *Phys. Rev. B*, 1988, vol. 37, No. 10, p. 5852.
2. Zhong W.I., Jiang B.I., Zhang P.L., Ma J.M., Cheng H.M., Yang Z.H., Li L.X. // *J. Phys.: Condens. Matter*, 1993, vol. 5, No. 16, p. 2619.
3. Colla E.V., Fokin A.V., Koroleva E.Yu., Kumzerov Yu.A., Vakhrushev S.V., Savenko V.N. // *Nanostructured Materials*, 1999, vol. 12, p. 963.
4. Uchino K., Sadanaga E., Hirose T. // *J. Amer. Ceram. Soc.*, 1989, vol. 72, No. 8, p. 1555.
5. Vysochanskii Yu.M., Slivka V.Yu. // *Uspekhi Fiz. Nauk*, 1992, vol. 162, No. 2, p. 139 (in Russian).
6. Cho Y.W., Choi S.K., Vysochanskii Yu.M. // *J. Mater. Res.*, 2001, vol. 16, No. 11, p. 3317.
7. Hlinka J., Gregora I., Vorliček V. // *Phys. Rev. B.*, 2002, vol. 65, No. 6, p. 064308 (and references therein).
8. Hayashi S., Yamamoto K. // *Superlattices and Microstructures*, 1986, vol. 2, No. 5, p. 581.

9. Campbell I.H., Fauchet P.M. // Sol. State Commun., 1986, vol. 58, No. 10, p. 739.
10. Roy A., Sood A.K. // Phys. Rev. B., 1996, vol. 53, No. 18, p. 12127.
11. Grabar A.A., Vysochanskii Yu.M., Slivka V.Yu. // Fiz. Tverd. Tela, 1984, vol. 26, No. 10, p. 3086 (in Russian).
12. Yevych R.M., Rushchanskii K.Z., Mitrovcij V.V. Lattice dynamics and chemical bonding in $\text{Sn}_2\text{P}_2\text{S}_6$ crystals: calculations and experiments. – In: Abstr. VI Ukrainian-Polish and II East-European Meeting on Ferroelectrics Physics. Uzhgorod-Synjak, Ukraine, 6–10 September 2002, p. 104.
13. Gomonnai A.V., Grabar A.A., Vysochanskii Yu.M., Belayev A.D., Machulin V.F., Gurzan M.I., Slivka V.Yu. // Fiz. Tverd. Tela, 1981, vol. 23, No. 12, p. 2093 (in Russian).
14. Selke W., Fisher M.E. // Phys. Rev. B, 1979, vol. 20, No. 1, p. 257; Selke W. // Physics Reports, 1988, vol. 170, p. 213; Neubert B., Pleimling M., Siems R. // Ferroelectrics, 1998, vol. 208–209, p. 141.
15. Pleimling M. // Phys. Rev. B, 2002, vol. 65, No. 18, p. 184406.

Вплив розмірного фактору на фазовий перехід у кристалах $\text{Sn}_2\text{P}_2\text{S}_6$: експериментальні результати та розрахунок у моделі ANNNI

О.В.Дробнич¹, О.О.Молнар¹, О.В.Гомоннай²,
Ю.М.Височанський¹, І.П.Пріц¹

¹ Ужгородський національний університет,
88000 Ужгород, вул. Підгірна, 46

² Інститут електронної фізики НАН України,
88000 Ужгород, вул. Університетська, 21

Отримано 18 жовтня 2002 р., в остаточному вигляді –
21 квітня 2003 р.

Досліджується вплив розмірного ефекту на фундаментальні властивості сегнетоелектрика $\text{Sn}_2\text{P}_2\text{S}_6$. У спектрах раманівського розсіювання мікрокристалічного порошку $\text{Sn}_2\text{P}_2\text{S}_6$ спостерігається зменшення частоти, зростання ширини та поява асиметрії лінії. Теоретичні розрахунки, виконані в моделі ANNNI для мікрокристалів $\text{Sn}_2\text{P}_2\text{S}_6$ різного розміру, передбачають пониження температури сегнетоелектричного фазового переходу зі зменшенням характеристичного розміру.

Ключові слова: мікрокристали, розмірні ефекти, комбінаційне розсіювання, ANNNI модель

PACS: 36.40.Ej, 63.22.+m